

Evolution of Dipole-Type Blocking Life Cycles: Analytical Diagnoses and Observations

Fei Huang^{1,2,3}, Xiaoyan Tang^{1,3}, S. Y. Lou^{1,3} and Cuihua Lu⁴

¹*Department of Physics, Shanghai Jiao Tong University, Shanghai, 200030, China*

²*Physical Oceanography Laboratory, Department of Marine Meteorology,
Ocean University of China, Qingdao, 266003, China*

³*Center of Nonlinear Science, Ningbo University, Ningbo, 315211, China*

⁴*Weather Bureau of Zaozhuang, Zaozhuang, 277148, China*

Abstract

A variable coefficient Korteweg de Vries (VCKdV) system is derived by considering the time-dependent basic flow and boundary conditions from a nonlinear, inviscid, nondissipative, and equivalent barotropic vorticity equation in a beta-plane. One analytical solution obtained from the VCKdV equation can be successfully used to explain the evolution of atmospheric dipole-type blocking (DB) life cycles. Analytical diagnoses show that background mean westerlies have great influence on evolution of DB during its life cycle. A weak westerly is necessary for blocking development and the blocking life period shortens, accompanied with the enhanced westerlies. The shear of the background westerlies also plays an important role in the evolution of blocking. The cyclonic shear is preferable for the development of blocking but when the cyclonic shear increases, the intensity of blocking decreases and the life period of DB becomes shorter. Weak anticyclonic shear below a critical threshold is also favorable for DB formation. Time-dependent background westerly (TDW) in the life cycle of DB has some modulations on the blocking life period and intensity due to the behavior of the mean westerlies. Statistical analysis regarding the climatological features of observed DB is also investigated. The Pacific is a preferred region for DB, especially at high latitudes. These features may associate with the weakest westerlies and the particular westerly shear structure over the northwestern Pacific.

PACS numbers: 47.32.-y; 47.35.-i; 92.60.-e; 02.30.Ik

I. INTRODUCTION

Atmospheric blocking is an important large-scale weather phenomena at mid-high latitudes in the atmosphere that has a profound effect on local and regional climates in the immediate blocking domain (Rex 1950a,b; Illari 1984) as well as in regions upstream and/or downstream of the blocking event (Quiroz 1984; White and Clark 1975). Therefore, it has long been of interest to synoptic and dynamical meteorologists. The formation, maintenance and collapse of atmospheric blocking always cause large-scale weather or short-term climate anomalies. Hence, the prediction for atmospheric blocking plays a significant role in regional midterm weather forecast and short-term climate trend prediction. Because of the needs of midterm weather forecast, there are has been a lot of research on dynamics of blocking. However, the physical mechanism leading to blocking formation remains unclear, which may result in the difficulty of blocking onset prediction using general circulation models (Tracton et al. 1989; Tibaldi and Molteni 1990).

Theoretical (Long 1964; Charney and DeVore 1979; Tung and Linzen 1979; McWilliams 1980; Malguzzi and Malanotte-Rizzoli 1984; Haines and Marshall 1987; Butchart et al. 1989; Michelangeli and Vautard 1998; Haines and Holland 1998; Luo 2000; Luo et al. 2001), observational (Rex 1950a,b; Colucci and Alberta 1996; Berggren et al. 1949; Illari 1984; Quiroz 1984; White and Clark 1975; Dole and Gordon 1983; Dole 1986, 1989; Lejenänd Øland 1983; Lupo and Smith 1995a), and numerical (Tanaka 1991, 1998; Luo et al. 2002; DAndrea et al. 1998; Ji and Tibaldi 1983; Chen and Juang 1992; Colucci and Baumhefner 1998) studies on the atmospheric blocking systems have undergone substantial and extensive development over the past several decades. Usually an atmospheric blocking anticyclone has three type of patterns: monopole-type blocking (or Ω -type blocking), dipole-type blocking (McWilliams 1980; Malguzzi and Malanotte-Rizzoli 1984; Luo and Ji 1991), and multipole-type blocking (Berggren et al. 1949; Luo 2000). The setup of the two later patterns are usually due to the strong nonlinear interaction between upstream high frequency synoptic-scale transient eddies and planetary-scale waves in exciting blocking circulation (Hansen and Chen 1982; Shutts 1983, 1986; Ji and Tibaldi 1983; Illari and Marshall 1983; Illari 1984; Hoskins et al. 1985; Egger et al. 1986; Mullen 1987; Holopainen and Fortelius 1987; Haines and Marshall 1987; Vautard and Legras 1988; Vautard et al. 1988; Chen and Juang 1992; Tanaka 1991; Lupo and Smith 1995b; Lupo 1997; Lupo and Smith 1998; Haines and Holland

1998; Luo 2000, 2005a,b). However, the nature of the planetary-synoptic scale interaction has yet to be clarified theoretically (Colucci 1985, 1987).

Atmospheric blocking events, mainly located in the mid-high latitudes and usually over the ocean, were first discovered as a dipole pattern by Rex (1950a,b). Later, Malguzzi and Malanotte-Rizzoli (1984) first found the dipole-type blocking from the Korteweg-de Vries (KdV) Rossby soliton theory. However, their analytical results cannot explain the onset, developing and decay of a blocking system. Recently, Luo et al. (2001) proposed the envelope Rossby soliton theory based on the deduced nonlinear Schrödinger (NLS) type equations to explain the blocking life cycle. However, they only obtained their solutions of the NLS type equations numerically instead of analytically.

In 1895, the KdV equation was firstly derived in the classic paper of Korteweg and de Vries (1895) as a fundamental equation governing propagation of waves in shallow water. After that, much progress has been made on this equation in both mathematics and physics. Now, physical applications of the KdV equation have been seen in a number of problems such as plasmas (Zabusky and Kruskal 1965; Rao et al. 1990), quasi-one-dimensional solid-state physics (Flytzanis et al. 1985), nonlinear transmission lines (Yoshinaga and Kakutani 1984), and so on.

In all these applications, the KdV equation arises as an approximate equation valid in a certain asymptotic sense. Taking account of additional physical factors, one may also obtain various KdV-type equations. For instance, a variable coefficient KdV-type (VCKdV) equation with conditions given at the inflow site was derived as governing the spatial dynamics in a simplified one-dimensional model for pulse wave propagation through fluid-filled tubes with elastic walls (Flytzanis et al. 1985), nonlinear transmission lines (Yoshinaga and Kakutani 1984), and so on. From the discussion below of a problem on the dynamics of atmospheric blockings, it will be seen that VCKdV equation is fairly universal and useful to explain the lifetime of the atmospheric blocking systems.

One important fact is that in the usual treatment of deriving either KdV- or NLS-type equations in the study of atmospheric blocking dynamics, one always separates the background flow, assumed to linearly depend on y only, and takes zero boundary values. Nonetheless, in reality, the background westerly changes with time as well as the shear type, which is something that has not yet been considered. Therefore, in this paper, we are motivated to introduce time into the background flow and boundary conditions to reinvestigate the

Rossby KdV theory for atmospheric blocking systems.

The term “blocking” denotes a breakdown in the prevailing tropospheric westerly flow at midlatitudes, often associated with a split in the zonal jet and with persistent ridging at higher latitudes (Rex 1950a,b; Illari 1984). Therefore, the basic pattern of blocking is dipole type and it always occurs under weak background westerlies (Shutts 1983; Luo and Ji 1991; Luo 1994; Luo et al. 2001; Luo 2005b). Weak background westerlies as a precondition for block onset were first noted by Shutts (1983), who found that the block does not occur for more rapid flows in which a stationary free state cannot be excited. However, Tsou and Smith (1990) and Colucci and Alberta (1996) suggested that the preconditioned planetary-scale ridge (incipient blocking ridge) may be another necessary condition for block onset in addition to the weak planetary-scale westerly flow.

Although previous theoretical analysis have shown that the weaker background westerlies were prevailing for the onset of DB than that of Ω -type blocking (Luo 1994), the role of the weak westerlies on the evolution of DB life cycle is still unclear. Further, how variations of the time-depend background westerlies influence the evolution of DB during its life period is also an interesting problem, since the realtime westerlies vary with time. Shear in the background westerlies was always introduced into theoretical models (Tung and Linzen 1979; McWilliams 1980; Malguzzi and Malanotte-Rizzoli 1984; Haines and Marshall 1987; Butchart et al. 1989; Luo 1994; Haines and Holland 1998; Luo et al. 2001) in the study of blocking, while Luo (1995) revealed that dipole structure of solitary Rossby waves excited by the β parameter could be obtained excluding the effect of shearing basic-state flow. In addition, the role of anticyclonic shear of basic-state flow on DB was emphasized (Luo 1994). In contrast, Luo et al. (2001) found that the cyclonic shear of the background westerly wind at the beginning of block onset was a favorable preblock environment, which increased the strength of the precursor blocking ridge, but the anticyclonic shear weakened the precursor blocking ridge considerably. Recently, Luo (2005b) also found that the asymmetry, intensity, and persistence of dipole block depend strongly upon the horizontal shear of the basicstate flow prior to block onset. Then there arises another question: what does the role of cyclonic/anticyclonic shear of the background westerlies play in the evolution of DB during different stages of its life cycle?

In this paper, we will focus on the two questions mentioned above by diagnosing the analytical solution obtained from a VKdV equation derived from the atmospheric nonlinear,

inviscid, nondissipative, and equivalent barotropic vorticity equation in a beta plane considering the time-dependent background flow and boundary conditions. The paper is organized as follows. Section 2 introduces the derivation of the VCKdV equation and its analytical solution. Analytical diagnosis of background westerly variations (including the variation of mean flow, westerly shears, and the time-dependent background flow) on the evolution of DB during its life cycle are investigated in Section 3. In the following section, some statistical observational results about DB in the Northern Hemisphere are given and possible interpretations from above theoretical model are demonstrated. Section 5 will outline our conclusions.

II. THEORETICAL MODEL

A. Derivation of the VCKdV equation

Our starting model is the atmospheric nonlinear, inviscid, nondissipative, and equivalent barotropic vorticity equation in a beta-plane channel (Pedlosky 1979; Luo 2001, 2005a):

$$(\partial_t + u\partial_x + v\partial_y)(v_x - u_y - F\psi) + \beta\psi_x = 0, \quad (1)$$

which is well known and one of the most important models in the study of atmospheric and oceanic dynamical systems. In equation (1), $u = -\psi_y$, $v = \psi_x$, ψ is the dimensionless stream function, u and v are components of the dimensionless velocity, $F = L^2/R_0^2$ is the square of the ratio of the characteristic horizontal length scale L to the Rossby deformation radius R_0 , $\beta = \beta_0(L^2/U)$, $\beta_0 = (2\omega_0/a_0)\cos\phi_0$, in which a_0 is the Earth's radius, ω_0 is the angular frequency of the earth's rotation, ϕ_0 is the latitude, and U is the characteristic velocity scale. The characteristic horizontal length scale can be $L = 10^6\text{m}$ and the characteristic horizontal velocity scale is taken as $U = 1\text{ms}^{-1}$.

Similar to the usual treatments, we rewrite the stream function as $\psi = \psi_0(y, t) + \psi'$ where ψ_0 means the background flow term, and introduce the stretched variables $\xi = \epsilon(x - c_0t)$, $\tau = \epsilon^3t$, (c_0 is a constant). In the previous studies, the background field ψ_0 is often taken only as a linear function of y , and in most cases one simply makes the expansion $\psi' = \sum_{n=1}^{\infty} \epsilon^n \psi'_n(\xi, y, \tau)$. However, here we also have the expansion for the background flow term as $\psi_0 = U_0(y) + \sum_{n=1}^{\infty} \epsilon^n U_n(y, \tau)$. Then, again similarly, substitute the expansions

into (1) and set the coefficient of each order of ϵ equal to zero. For notation simplicity, the primes are dropped out in the remaining of this paper. In the first order of ϵ , we obtain

$$\psi_1 = A(\xi, \tau)G(y, \tau),$$

where G is determined by

$$(U_{0y} + c_0)G_{yy} - (F^2c_0 + \beta + U_{0yyy})G = 0.$$

In the second order, we have

$$\psi_2 = A(\xi, \tau)G_1(y, \tau) + A^2(\xi, \tau)G_2(y, \tau),$$

where G_1 satisfies

$$(U_{0y} + c_0)^2G_{1yy} - (U_{0y} + c_0)(F^2c_0 + U_{0yyy} + \beta)G_1 - [(U_{0y} + c_0)U_{1yyy} - (F^2c_0 + U_{0yyy} + \beta)U_{1y}]G = 0,$$

and G_2 satisfies

$$2(U_{0y} + c_0)^2[(U_{0y} + c_0)G_{2yy} - (F^2c_0 + U_{0yyy} + \beta)G_2] + [(F^2c_0 + U_{0yyy} + \beta)U_{0yy} - (U_{0y} + c_0)U_{0yyy}]G^2 = 0.$$

Substituting the solutions obtained from the previous two orders and $\psi_3 = 0$ into the coefficient of the third order of ϵ , then integrating the result with respect to y from 0 to y_0 as in the usual treatments of the oceanic and atmospheric dynamics, yield the modified VCKdV equation ($e_2 \neq 0$) and/or VCKdV equation ($e_2 = 0$)

$$e_1 A_{\xi\xi\xi} + (e_2 A^2 + e_3 A + e_4) A_{\xi} + (e_5 A)_{\tau} + e_6 = 0, \quad (2)$$

with ($e_i \equiv e_i(\tau)$),

$$e_1 = \int_0^{y_0} -G(U_{0y} + c_0)dy,$$

$$e_2 = \int_0^{y_0} 2(G_{yyy}G_2 - G_y G_{2yy}) + GG_{2yyy} - G_{yy}G_{2y}dy,$$

$$e_3 = \int_0^{y_0} 2U_{1yyy}G_2 - 2U_{1y}G_{2yy} + G_{yyy}G_1 - (G_y G_{1y})_y + GG_{1yyy}dy,$$

$$e_4 = \int_0^{y_0} U_{1yyy}G_1 - G_{yy}U_{2y} + GU_{2yyy} - U_{1y}G_{1yy}dy,$$

$$e_5 = \int_0^{y_0} G_{yy} - F^2Gdy,$$

$$e_6 = \int_0^{y_0} (U_{1yy} - F^2U_1)_{\tau}dy.$$

B. Exact solution of the VCKdV equation

Obviously, in the above derivation of the VCKdV equation, the background flow is left as an arbitrary function of $\{y, t\}$. For the sake of obtaining meaningful analytical solutions to the VCKdV equation, we have to fix its variable coefficients further. In the expansion of the background flow term ψ_0 , if $U_n = 0$ for $n \geq 1$, it becomes a function of y as usual. Therefore,

the higher order items U_n can be viewed as higher-order corrections to the lowest one, U_0 . Because of this, we also take U_0 as a linear function of y ; that is, $U_0 = a_1 y + a_0$ with a_0, a_1 constant, and for the next higher order, as mentioned before, it is chosen as a quadratic function of y with time dependent coefficients; that is, $U_1 = a_2 y^2 + a_3 y + a_4$ with a_2, a_3, a_4 all time dependent functions. The higher orders are all taken as zero, namely $U_n = 0$ for $n \geq 2$ so as to simplify the problem. In this case, the background flow is similar to the cases in Gottwald and Grimshaw (1999) except that the mean flow configurations are time-varying instead of stable. It is noted that the quantity ϵa_2 plays the role of the shear of the background flow, and the background westerly wind is determined by $a_1 + \epsilon a_3$. Apparently, both the shear and the background westerlies vary with time. After these selections, G, G_1 and G_2 can be easily solved as

$$G = F_1 \sin(My + F_2),$$

$$G_1 = F_5 \sin(My + F_6) + \frac{(F^2 + M^2)F_1}{4M(a_1 F^2 - \beta)} [M(2a_2 y + a_3) \sin(My + F_2) - (2a_2 M^2 y^2 + 2a_3 M^2 y - a_2) \cos(My + F_2)],$$

$$G_2 = F_3 \sin(My + F_4),$$

where $c_0 = -\frac{a_1 M^2 + \beta}{F^2 + M^2}$. $F_1 \sim F_6$, and all functions with respect to time should be determined by the boundary conditions. No constraints are made on these functions because in the following, we will focus on the behavior of the VCKdV equation with different values for the parameters appeared in the background flow so as to investigate what effect of the background can make on the possible coherent structure; that is, the soliton solution.

With the above selections and results, we can finally write down an exact solution to the VCKdV equation as

$$A = \frac{C_2 \xi - H}{2C_3 e_6 \sqrt{-C_1 + C_2 \tau}} + \frac{(F^2 a_1 - \beta)^{1/3}}{e_6 (F^2 + M^2)^{2/3} \sqrt{-C_1 + C_2 \tau}} \left\{ \frac{C_4}{C_3^2 C_7^{1/3}} + 12C_3 K^2 C_7^{2/3} \operatorname{sech}^2 \left[\frac{8K^3 C_3^3 C_7 - 2KC_4}{C_2 \sqrt{-C_1 + C_2 \tau}} + KC_5 - 4K^3 C_6 \right. \right. \\ \left. \left. + \frac{KC_3 C_7^{1/3} (F^2 + M^2)^{2/3}}{2(F^2 a_1 - \beta)^{1/3}} \left(\frac{2\xi}{\sqrt{-C_1 + C_2 \tau}} + \int \frac{H}{(-C_1 + C_2 \tau)^{3/2}} d\tau \right) \right] \right\} - \frac{e_4 \sqrt{-C_1 + C_2 \tau}}{C_3 e_6^2}, \quad (3)$$

$$\text{where } H = \int \frac{2(C_1 - C_2 \tau)(e_4 e_6 \tau - e_4 \tau e_6)}{e_6^2} + 2e_7 C_3 \sqrt{C_2 - C_1 \tau} - \frac{e_4 C_2}{e_6} d\tau,$$

$$e_4 = [2a_2 \sin(My_0 + F_6) - 2a_2 \sin(F_6) - M(2a_2 y_0 + a_3) \cos(My_0 + F_6) + Ma_3 \cos(F_6)] F_5 - \frac{(F^2 + M^2)F_1}{4(F^2 a_1 - \beta)M} [a_2 a_3 \sin(F_2) M - (M^2 a_3^2 + 2a_2^2)(\cos(My_0 + F_2) - \cos(F_2)) + M(2a_2 y_0 + a_3)(2M^2 a_2 y_0^2 +$$

$$2M^2 a_3 y_0 - a_2) \sin(My_0 + F_2)]],$$

$$e_6 = -\frac{F_1(M^2+F^2)}{M}[\cos(F_2) - \cos(My_0 + F_2)],$$

$$e_7 = -\frac{y_0}{6}[(2y_0^2 F^2 - 12)a_{2\tau} + 3y_0 F^2 a_{3\tau} + 6F^2 a_{4\tau}],$$

and $M, K, C_i, (i = 1, 2, \dots, 7)$ are arbitrary constants. There is also a necessary relation between $F_2 \sim F_4$:

$$F_3[2M^2(\lambda_0^2 a_1 - \beta)\sqrt{-C_1 + C_2\tau}(2a_2 \sin(F_4) - 2a_2 \sin(My_0 + F_4) - a_3 M \cos(F_4) + M(2y_0 a_2 + a_3) \cos(My_0 + F_4))] - F_1^2(F^2 + M^2)[a_2 M^3 \sqrt{-C_1 + C_2\tau}(\cos(F_2) \sin(F_2) - \cos(My_0 + F_2) \sin(My_0 + F_2) + My_0) - C_3(F^2 a_1 - \beta)(F^2 + M^2)(\cos(F_2) - \cos(My_0 + F_2))^2] = 0.$$

III. ANALYTICAL DIAGNOSIS ON DB EVOLUTION

In this section we analyze a DB evolution case under certain parameters. Set $e_4 = 0$ and $a_4 = -\frac{y_0}{2}a_3 + (\frac{2}{F^2} - \frac{y_0^2}{3})a_2$ (and then $e_6 = 0$). Hence, one possible approximate solution to (1) is in the form of

$$\begin{aligned} \psi \approx & \epsilon a_2 y^2 + (a_1 + \epsilon a_3)y + a_0 - \frac{y_0}{2}\epsilon a_3 + \left(\frac{2}{F^2} - \frac{y_0^2}{3}\right)\epsilon a_2 \\ & - \frac{\sin(My + F_2)}{[\cos(F_2) - \cos(My_0 + F_2)]} \times \frac{\epsilon M}{(M^2 + F^2)\sqrt{-C_1 + \epsilon^3 C_2 t}} \left\{ \frac{\epsilon C_2}{2C_3}(x - c_0 t) \right. \\ & + \frac{C_4 M_1}{C_3^2 C_7^{1/3}} + 12C_3 M_1 K^2 C_7^{2/3} \times \text{sech}^2 \left[\frac{K}{\sqrt{-C_1 + \epsilon^3 C_2 t}} \left(\frac{\epsilon C_3 C_7^{1/3}}{M_1}(x - c_0 t) \right. \right. \\ & \left. \left. + \frac{8K^2 C_3^3 C_7 - 2C_4}{C_2} \right) + K(C_5 - 4K^2 C_6) \right] \left. \right\}, \end{aligned} \quad (4)$$

$$\text{with } M_1 = \frac{(F^2 a_1 - \beta)^{1/3}}{(F^2 + M^2)^{2/3}}.$$

From the analytical solution of streamfunction ψ it is easily to derive the background westerly flow $\bar{u} = -\frac{\partial \psi_0}{\partial y} = \bar{u}_0 + \delta y$, where $\bar{u}_0 = -(a_1 + \epsilon a_3(t))$ and $\delta = -2\epsilon a_2(t)$. As we known, the weather or climate periodically changes on either large or small scales. Thus, it is reasonable to choose the time-dependent unknown functions in the background flow as periodic, so the sine function is in use. Thus we choose $a_2(t) = -a_{20} \sin(k_2 t)$, $a_3(t) = -a_{30} \sin(k_3 t)$. The basic-state westerlies have cyclonic shear when $\delta < 0$ or $a_{20} > 0$, but correspond to anticyclonic westerly shear when $\delta > 0$ or $a_{20} < 0$. Here we consider $\phi_0 = 60^\circ N$ in that the blocking systems are mainly situated in the mid-high latitudes. For example, when we take the functions and parameters in our analytical solution (4) as $a_{20} = 0.1, k_2 = 2.1, a_{30} = 0.5, k_3 = k_2, F_2 = \arccos(10^{-8} \cosh(0.75t - 4.5)), \epsilon = 0.1, a_0 = 2, a_1 = -0.2, C_1 = -30, C_2 =$

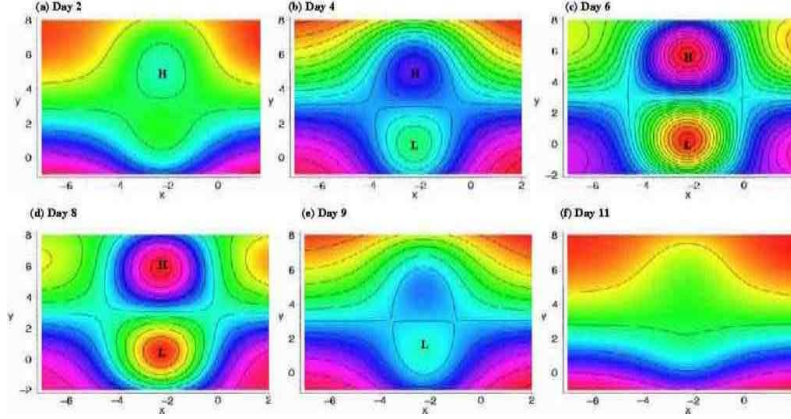


FIG. 1: A dipole blocking life cycle from the theoretical solution (4) with $a_2 = -0.1 \sin(2.1t)$, $a_3 = -0.5 \sin(2.1t)$, $\epsilon = 0.1$, $a_1 = -0.2$. The contour interval $CI=0.2$.

0.1, $C_3 = -10$, $C_4 = -16$, $C_5 = 4$, $C_6 = -7$, $C_7 = 0.1$, $K = 0.2$, $F = 64$, $M = \frac{\pi}{6}$, a dipole-type blocking life cycle appears and is shown in Fig. 1.

Figure 1 clearly reveals the onset, development, maintenance, and decay processes—a whole life cycle of a dipole-type blocking event. The streamlines are gradually deformed and split into two branches at the second day, with the anticyclonic high in the north developing first (Fig. 1a). Then the cut-off low develops south of the high, forming a pair of high-low dipole pattern where the center of the high is located at the higher latitude than that of the low (Fig. 1b). They are strengthened daily. At around the sixth day (Fig. 1c), they are at their strongest stage and then become weaker and eventually disappear after the eleventh day (Fig. 1d-f). Obviously, Fig. 1 possesses the phenomenon's salient features including their spatial-scale and structure, amplitude, life cycle and duration. Therefore, Fig. 1 is a very typical dipole-type blocking episode. More importantly, it corresponds quite well to a real observational blocking case (Fig. 2) that happened over the Pacific during 2-12 January 1996, which is obtained from the National Centers for Environmental Prediction-National Center for Atmospheric Research (NCEP-NCAR) reanalysis data. Because blocking is a large-scale atmospheric phenomenon, the geopotential height fields in Fig. 2 were filtered by preserving wave numbers 0-4 in a harmonic analysis around latitudes in order to filter high-frequency synoptic-scale perturbations.

It is easily found in Fig. 2 that the life cycle of this blocking lasts almost 10 days, experiencing three stages: onset (2-5 January, 1996), maturity (7-9 January, 1996) and decay (10-12 January, 1996). This blocking event developed within an atmospheric long Rossby

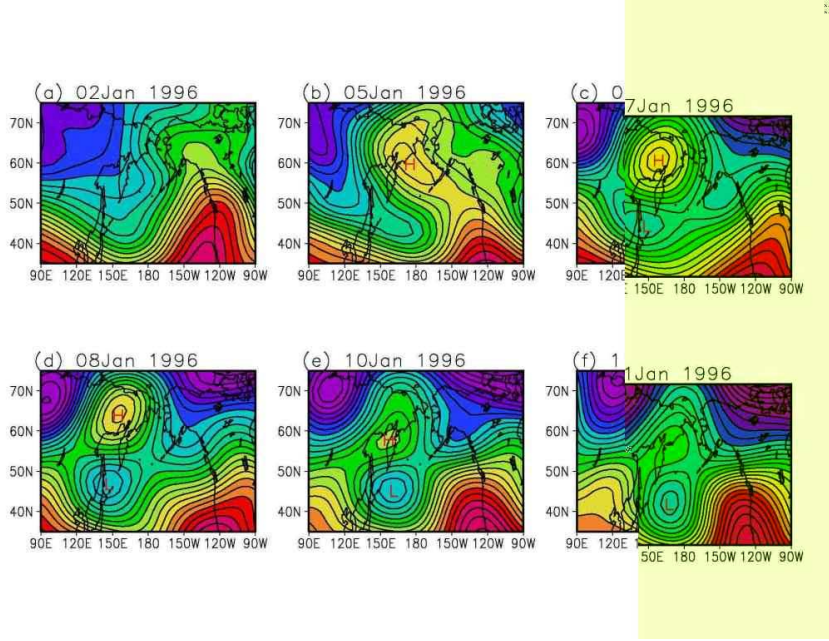


FIG. 2: Filtered geopotential height at 500-hPa pressure level of a blocking case during 2-11 Jan 1996. Contour interval is 4 gpm. The x -axis is longitude, and the y -axis is latitude.

wave ridge extending northwestward and an upstream cutoff low moving southeastward (Fig. 2a, b). With the strengthening of the blocking high and the cutoff low, two closed centers of high and low appeared forming a north-south dipole-like pattern with the closed high in the north and the closed low in the south during the mature stage (Fig. 2c, d). Then the high center decayed and vanished first, as well as the cutoff low decayed subsequently (Fig. 2e,f). At last the block became a travelling Rossby wave ridge and moved eastward (figure omitted).

A. Effect of the mean background westerlies

Previous research showed that the background westerlies are a necessary precondition for the onset of anticyclonic blocking and they also played an important role in the blocking life cycle (Shutts 1983, 1986; Luo and Ji 1991; Luo 1994; Luo et al. 2001). For DB evolution during its life cycle, the role of the mean background westerlies in the DB evolution is not clear in a VCKdV soliton system, while the typical KdV Rossby soliton can only represent a steady-state DB pattern instead of an evolution of DB life cycles. To simplify the question, here only variation of the mean flow is considered without westerly shear

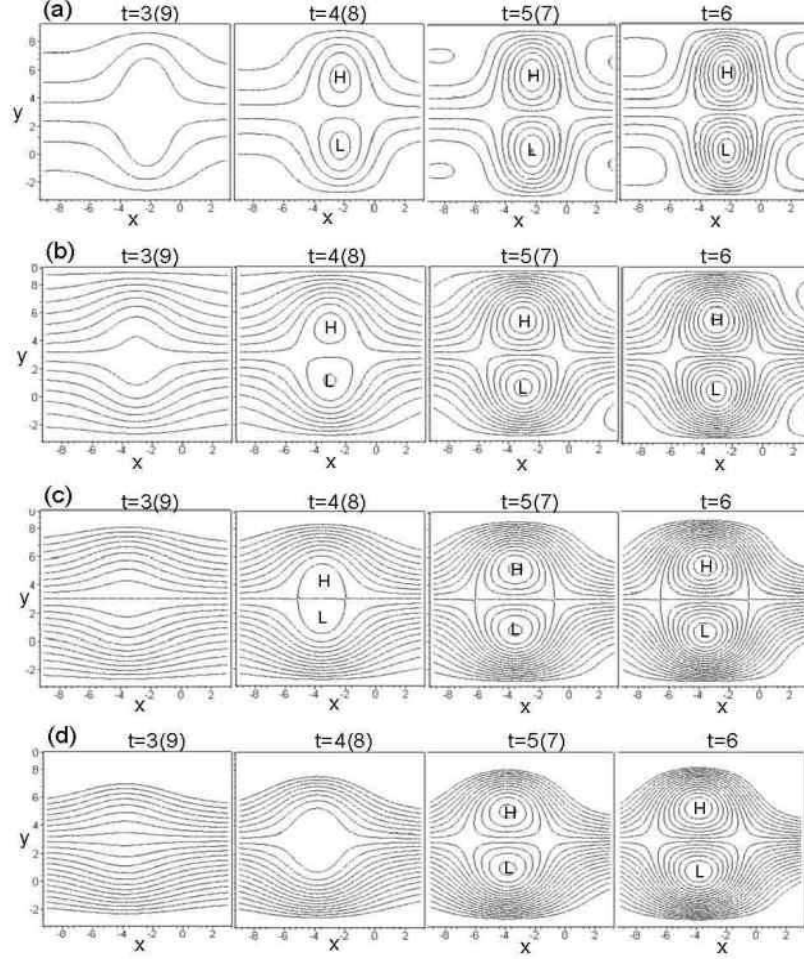


FIG. 3: The evolutions of DB life cycles under different background westerlies (a) $a_1 = -0.2$; (b) $a_1 = -0.5$; (c) $a_1 = -0.8$; (d) $a_1 = -1.0$. CI=0.4.

($a_2(t) = 0$) and time-dependent background westerly term ($a_3(t) = 0$). Only the parameter a_1 varies in different constants indicating the variation of the mean background westerlies. The evolutions of DB life cycles under different mean background westerlies are shown in Fig. 3.

It is shown in Fig. 3 that the intensity, zonal and meridional scales, position, and period of DB during its life episode alter with the increasing mean background westerlies. Under

the weak mean westerly $a_1 = -0.2$ condition (Fig. 3a), the DB period is about 10 days from $t = 1$ to $t = 10$, consistent with typical period of blocking observed [? ? ? ? ? ? ?]. At time $t = 2$ an incipient dipole-like envelop Rossby soliton pattern appears and begins to enhance, forming closed high and low centers at $t = 4$. Then the high and low centers strengthen dramatically from $t = 4$ to $t = 6$ and reach their peaks at $t = 6$. Subsequently, the high and low centers in DB decrease gradually from $t = 7$ to $t = 10$. The meridional scale of DB (distance between the high and low centers) increases during the developing period ($t = 1$ to $t = 6$) of DB life cycle and decreases during the decay process ($t = 7$ to $t = 10$). It is noticeable that the high and low centers in the DB streamlines pattern seem antisymmetric along the north-south direction as well as the evolution process is symmetric with respect to the mature phase of DB at $t = 6$ under the high idealized theoretical solution. However, the main characters of the DB streamlines pattern and its evolution, including the onset, development, mature, and decay processes, are well captured.

Comparing the DB evolution processes under different mean westerlies (Fig. 3b-d), it is easily found that the incipient dipole-like envelop at time $t = 3$ weakens with the mean westerly increasing. The closed streamlines of high and low centers in DB under weak westerly conditions (Fig. 3a,b) at $t = 4$ disappear and are replaced by the gradually decreasing envelop streamline pattern (Fig. 3c,d) when the parameter a_1 varies from $a_1 = -0.8$ to $a_1 = -1.0$. That means the period of the DB life cycle shortens when the mean westerlies increas. At time $t = 4$ or $t = 8$, it is very clear that the DB intensity represented by values of the DB high and low centers also weakens with the mean flow increasing. This feature is also clearly seen in Fig. 4, showing the intensity of DB high (Fig. 4a) and low (Fig. 4b) center varying with respect to time t . It is obvious that the high center of DB weakens while the low center strengthens when the mean westerlies increas throughout the period of DB life cycles. Nevertheless, the behaviors of the high and low centers appear inconsistent during the different developing stages of DB life episode. That is, the high center (Fig. 4a) decreases greatly during the onset ($t = 1$ to $t = 4$) and decay ($t = 8$ to $t = 11$) stages of DB life episode, and decreases slowly in the DB mature phase ($t = 5$ to $t = 7$). On the contrary, the low center (Fig. 4b) deepens greatly during the mature stage of DB life cycle, but strengthens relatively slightly at the onset and decay stages.

To see more clearly the movement of DB high center with respect to time t , Fig. 5 shows space-time ($x - t$ or $y - t$) cross sections crossing the high center. From the $x - t$

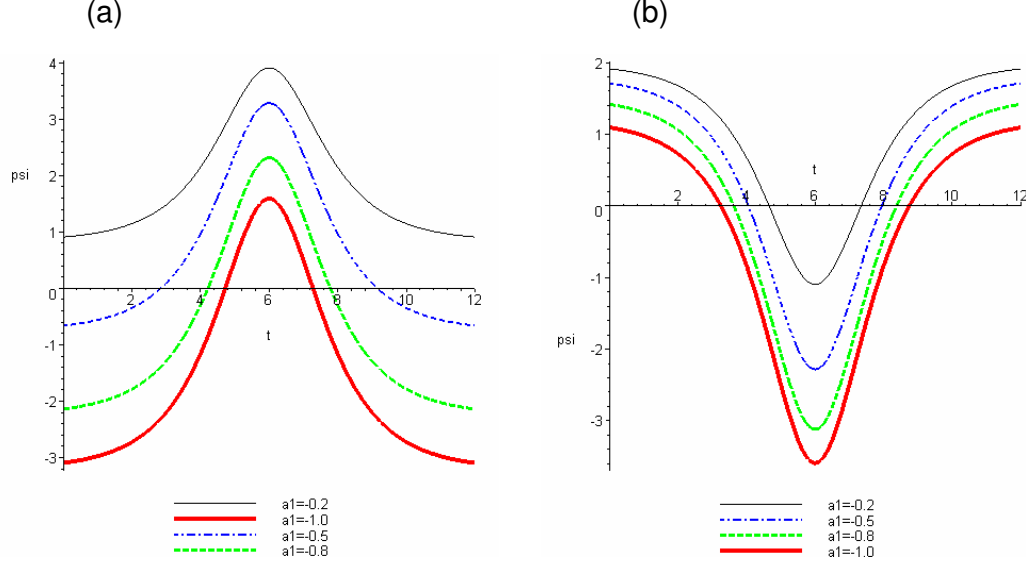


FIG. 4: The intensity of the DB high (a) and low (b) center varying with respect to time t .

cross section (Fig. 5a) it is found that the blocking high moves westward and the zonal scale of DB enlarges with the strengthening of the mean westerlies. This feature can also be identified in Fig. 3. For the $y - t$ cross section crossing the high center (Fig. 5b), the meridional scale of the DB shortens and the evolution crossing the dipole high/low center with respect to t displays a shrinking dipole-like pattern, suggesting shortening of DB period of life cycles under the condition of the mean westerlies increasing. This result implies that the DB could not maintain stationary long time in strong westerlies (Shutts 1983).

B. Effect of the background westerly shear

In this section effects of the westerly shears including cyclonic shear and anticyclonic shear on evolution of DB are investigated. As mentioned above, the westerly shear parameter δ is expressed as $\delta = -2\epsilon a_2(t)$; $\delta < 0$ or $a_2(t) > 0$ denotes the cyclonic background westerly shear, and $\delta > 0$ or $a_2(t) < 0$ represents the anticyclonic shear. As we know, $a_2(t)$ is a function with respect to time t . To simplify the question, here a_2 is assumed to be a small constant, suggesting a time-independent weak linear shear superposed on the back-

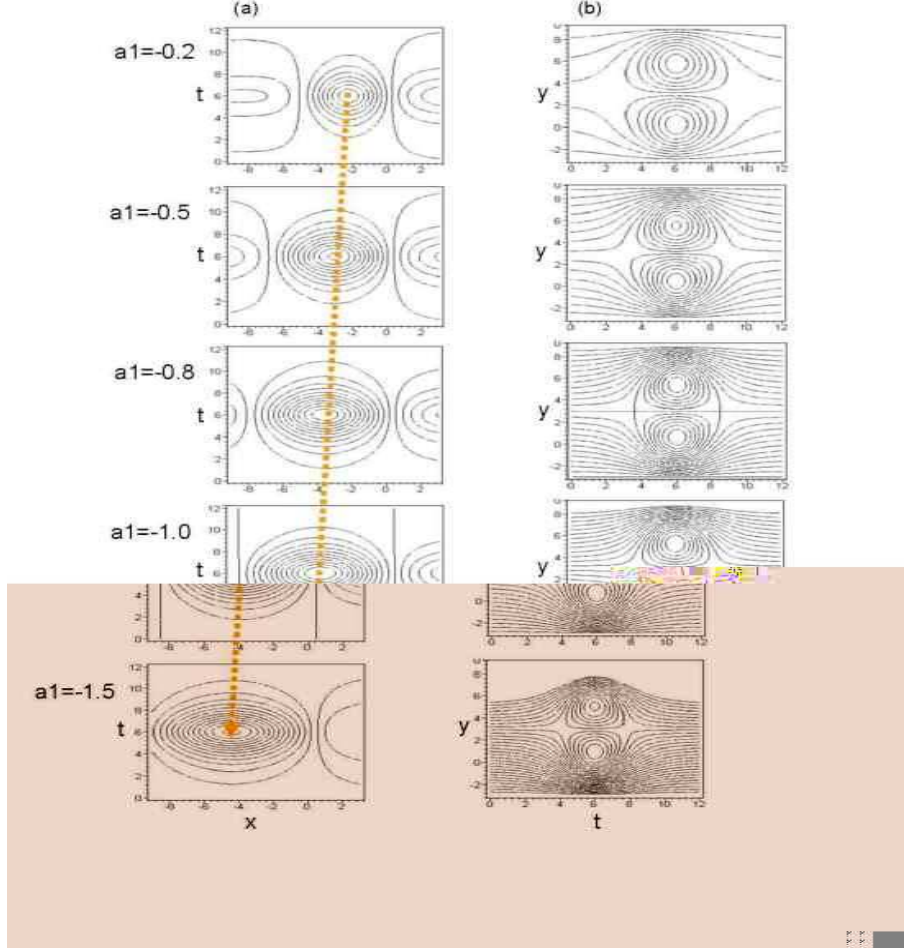


FIG. 5: The space-time $x - t$ (a) and $y - t$ (b) cross sections crossing the high center of DB under different basic mean westerlies. $CI=0.2$.

ground mean flow. The mean westerlies without the time-dependent term ($a_3(t) = 0$) is also assumed. Consequently, the background westerly with linear shear is $\bar{u} = \bar{u}_0 + \delta y$, where the mean flow $\bar{u}_0 = -a_1 = 0.6$.

1. The cyclonic westerly shear

The background westerly shear is always introduced into a theoretical model (Tung and Linzen 1979; McWilliams 1980; Malguzzi and Malanotte-Rizzoli 1984; Haines and Marshall 1987; Butchart et al. 1989; Luo 1994; Haines and Holland 1998; Luo et al. 2001; Luo 2005b)

in the study of blocking, but the role of the cyclonic westerly shear (CWS) in evolution of DB during its life cycle is not clear, although Luo et al. (2001) and Luo (2005b) emphasized the important role of the cyclonic shear of background westerly wind in block onset. Recently, Dong and Colucci (2005) also demonstrated the important effect of cyclonically sheared flow on forcing weakening westerlies associated with the Southern Hemisphere blocking onset. To compare the influence of different cyclonic shear on a DB episode, the DB evolutions at parameter $a_2 = 0.03, 0.15, 0.3, 0.45$ and 0.6 , corresponding to 1%, 5%, 10%, 15% and 20% of the mean westerlies \bar{u}_0 , are investigated respectively in Fig. 6. Results show that weak CWS is favorable for the onset of DB, similar to the conclusion by Luo et al. (2001), Luo (2005b), and Dong and Colucci (2005). However, the DB life period shortens and the DB high/low centers weaken simultaneously when the weak CWS enhances during the evolution of DB episode (Figs. 7a, c). The intensity variation of the low center appears different behaviors, considering the CWS comparisons with and without shear (Fig. 4). That is, the low weakens along with increasing CWS (Fig. 7c), and strengthens with increasing background mean westerlies without shear (Fig. 4b). A noticeable phenomenon is that the CWS destroys the antisymmetric structure of the DB high/low poles. The low develops more slowly than the high at the DB onset stage ($t = 4$), while it trails off faster than the high during the decay period ($t = 8$) with the CWS increasing (Fig. 6). This feature is also indicated in Figs. 7a,c.

2. The anticyclonic westerly shear

Luo (1994) revealed that strong anticyclonic westerly shear (AWS) was disadvantageous for establishment of dipole-type blocking, but his solution could not interpret the onset and decay process of DB. Recently, Luo et al. (2001) and Luo (2005b) also pointed out that the anticyclonic background westerly shear weakened the precursor blocking ridge considerably; therefore, the formation of a blocking anticyclone was difficult. However, the role of the AWS on DB life cycles is not clear. In our model, the influence of different weak AWS on DB episode with parameters $a_2 = -0.03, -0.15, -0.3, -0.45$, and -0.6 , respectively, are compared with each other in Fig. 8. Results show that only very weak anticyclonic shear is more preferable for the onset and maintenance of DB, resulting longer life of DB (Figs. 8a-c). There exists a threshold value of a_2 limiting the anticyclonic shear that controls the

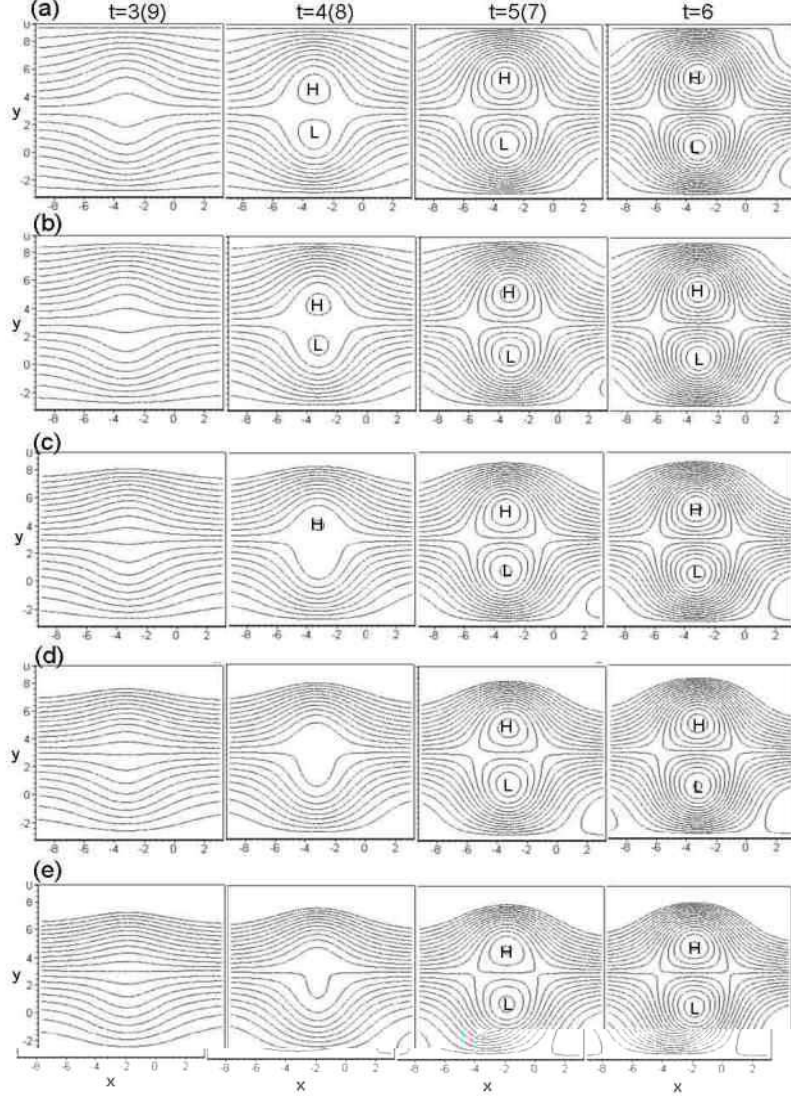


FIG. 6: The stream function patterns of DB evolution under different cyclonic westerly shears. (a) $a_2 = 0.03$; (b) $a_2 = 0.15$; (c) $a_2 = 0.3$; (d) $a_2 = 0.45$; (e) $a_2 = 0.6$. CI=0.4.

appearance of DB streamline patterns. Under the mean westerlies $\bar{u}_0 = 0.6$, the threshold of a_2 is about -0.45 , or the threshold shear $\delta_c = 0.09$, denoting the slope of lines on the $(\bar{u}_0 - y)$ plane. This means the DB is easily established under weak AWS condition when $\delta < \delta_c$. For $\delta < \delta_c$, the DB life period is prolonged obviously and DB establishes (decays) earlier (later) with the increasing of AWS (Figs. 8a-c). For $\delta > \delta_c$, the dipole-like circulation can still develop, but never be a blocking pattern splitting the westerlies into two northward and

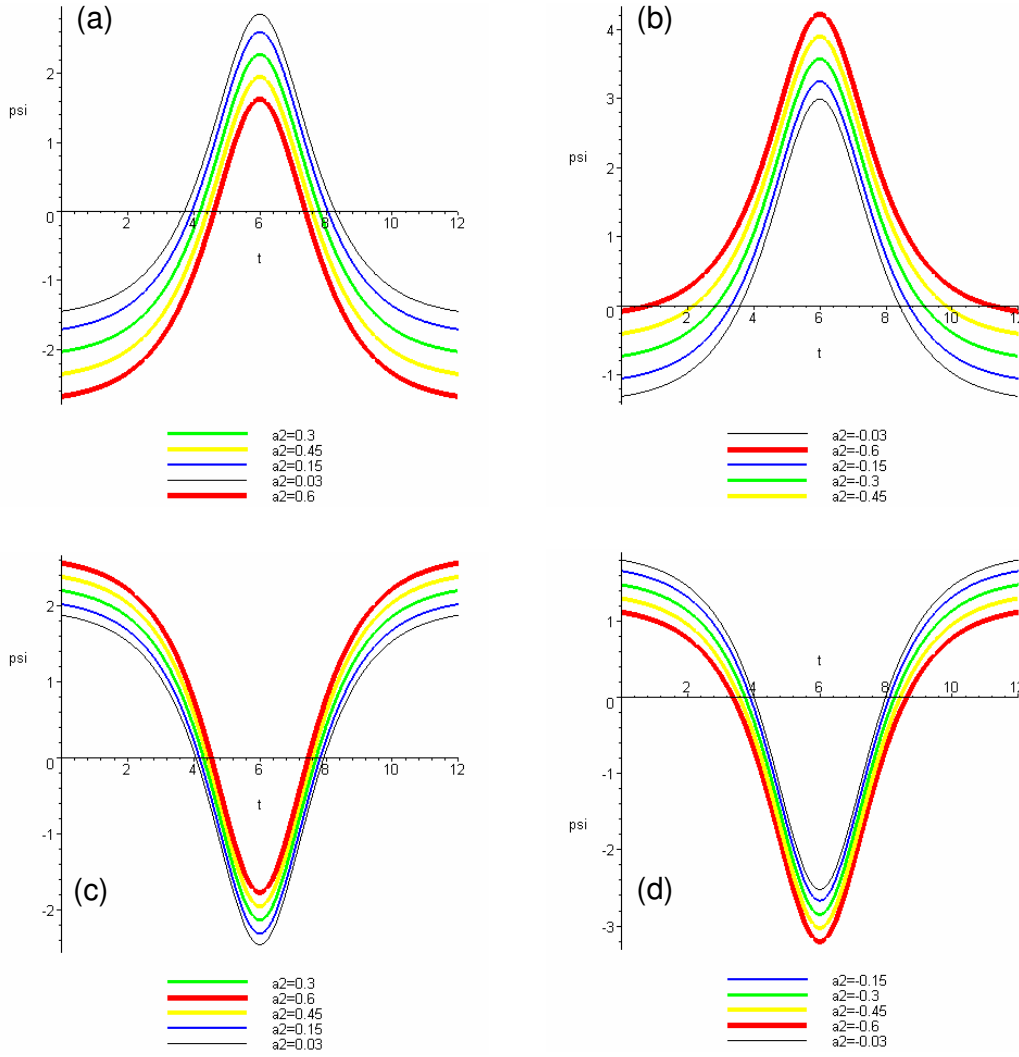


FIG. 7: The intensity of the DB high (a, b) and low (c, d) center varying with respect to time t under different conditions of westerly shears. (a) and (c) are for cyclonic shear, (b) and (d) are for anticyclonic shear.

southward branches (Figs. 8d,e). Instead, the separate northward westerlies around the high disappear and the developed high in the dipole comes from the most northern boundary, which indicates a cutoff high from the North Pole region moving southward, forming the dipole circulation together with the low in the south. Actually, in a daily synoptic chart, the cutoff high from the North Pole region is often seen moving southward. The threshold value of AWS decreases along with decreasing of the mean background westerlies \overline{u}_0 .

It is also obvious that the AWS induces the asymmetry development of the high/low centers in DB during different stages of its life cycle (Fig. 8). Especially at DB onset ($t = 3, 4$) and decay ($t = 8, 9$) phases, the high center is apparently stronger than the

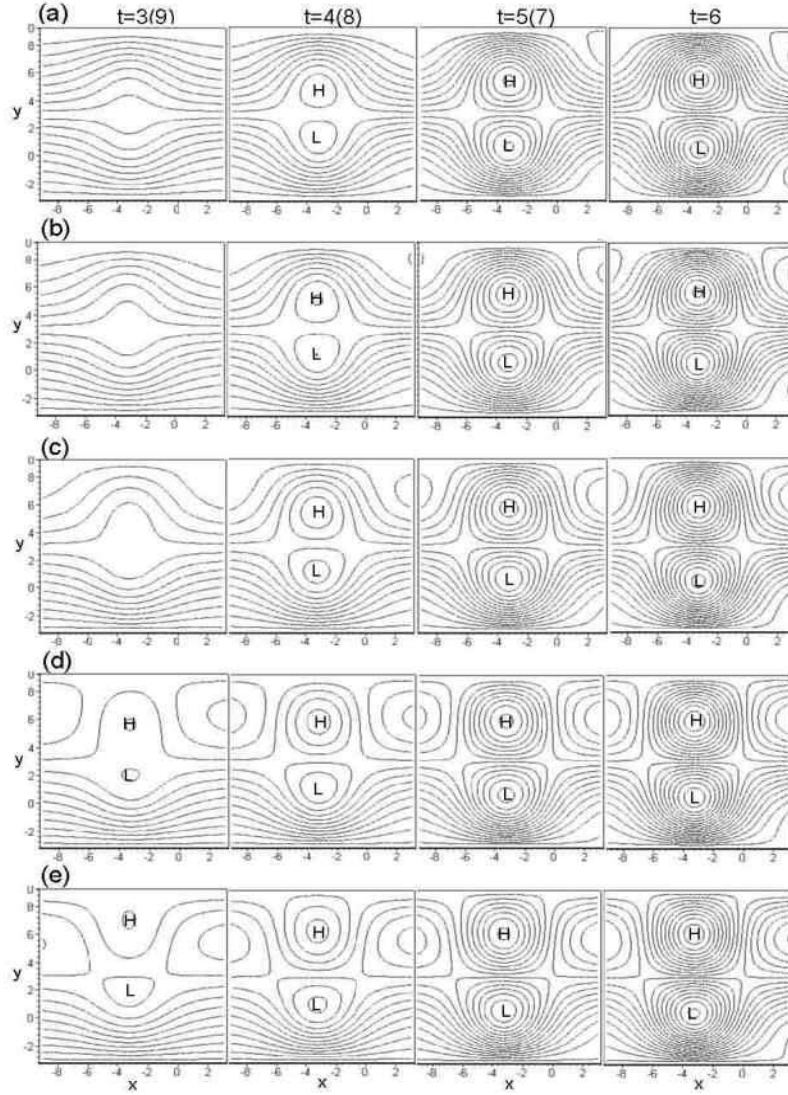


FIG. 8: The stream function patterns of DB evolution under different anticyclonic westerly shears.

(a) $a_2 = -0.03$; (b) $a_2 = -0.15$; (c) $a_2 = -0.3$; (d) $a_2 = -0.45$; (e) $a_2 = -0.6$. CI=0.4.

low center, and the high/low center tends to strengthen along with the strengthening of the AWS. The DB high/low center strengthens simultaneously when the AWS strengthens during the evolution of DB episode (Figs. 7b, d), which appears to have opposite behavior than that with CWS (Figs. 7a, c). In addition, the intensity of the DB dipole centers with AWS is stronger than that of CWS.

C. Effect of the time-dependent background westerlies

In the real atmospheric circulation, the background westerly is not always a constant during the life period of blocking. Actually there is interaction between blocking and the background westerlies; that is, the weak background westerlies modulated by transient eddies are a precondition for the onset of blocking; meanwhile, after the blocking is established, it prevents the westerlies passing through as a result of a weakened westerly (Berggren et al. 1949; Elliott and Smith 1949; Egger et al. 1986; Mullen 1987; Long 1964; Shutts 1983; Colucci 1985; Holopainen and Fortelius 1987; Dole 1989; Luo et al. 2001). Therefore, the background westerlies may be a time-dependent function during the episode interacting with blocking. For simplification, the westerly shear ($a_2 = 0$) is not considered here, so the background flow, $\bar{u} = \bar{u}_0 - \epsilon a_3(t)$, here is $\bar{u}_0 = -a_1 = 0.5$. Several types of $a_3(t)$ profiles shown in Fig. 9 are attempted to investigate the influence of time-dependent background westerlies (TDW) on DB evolution. Case 1 indicates the condition that the background westerlies become weakest at DB onset stage and increases gradually throughout the block life cycle. It is found that the variations of the curve slope do not impact the evolution of DB in Case 1. Case 2 and 3 show the westerly profiles reflecting the interaction between the background westerlies and blocking with the westerlies decreasing during the developing period before the DB peak at $t = 6$ and increasing throughout the decay stage after the DB peak. The latter is conceptually consistent with the actual variation of the westerlies during a blocking evolution (Elliott and Smith 1949).

Fig. 10 presents the intensity of the DB high (Fig. 10a) and low (Fig. 10b) center varying with respect to time t under different types of TDW as shown in Fig. 9 during the DB life cycle. For case 1, the TDW varying from the weakest to the strongest stage during the DB life cycle, shortens the life period of the DB and weakens the intensity of the DB. Tests changing slopes of the $(\bar{u} - t)$ profile indicate that variation rate of the background westerlies during the DB episode does not act as an influence on the DB evolution (Figures omitted). This result implies that the time-dependent westerlies varying accordantly before and after the DB reaching its peak phase play a similar role in the DB evolution. For the TDW reflecting interaction between blocking and background flow in case 2, the evolution of DB has been considerably impacted. The most noticeable feature is that the time of the DB onset and decay lags that without TDW term, either for the high (Fig. 10a) or for the

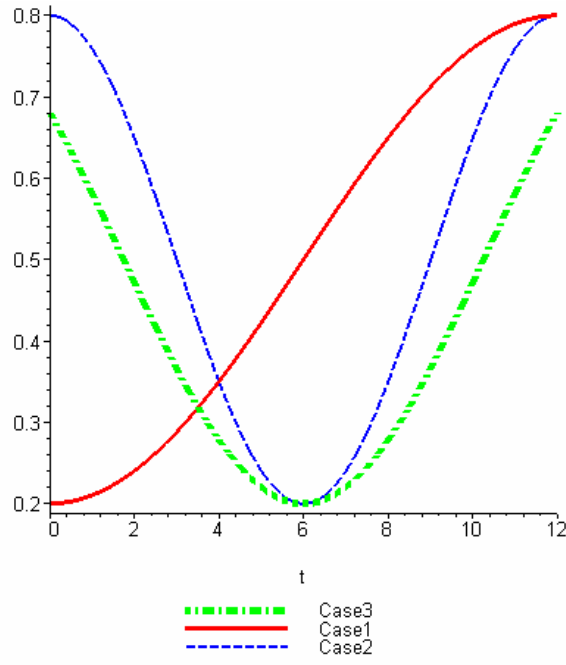


FIG. 9: Different types of TBW profiles during the DB life cycle. The x-axis is time t in DB life episode and y-axis denotes \bar{u} . Case1 represents $\bar{u} = 0.5 - 0.3\cos(0.26t)$, Case2 denotes $\bar{u} = 0.5 - 0.3\cos(0.52(t - 6))$, Case3 denotes $\bar{u} = 0.5 - 0.3\cos(0.37(t - 6))$.

low center (Fig. 10b) in the dipole structure. The decay process from the peak phase of DB to its disappearance is longer than the DB developing process from the onset of DB to its peak phase, resulting in the asymmetric evolution of the DB during its life episode. In addition, the intensity of the DB high/low centers at its peak phase strengthens slightly. However, the intensity of DB depends on the slope of the profile. For example, when the slope is not so sharp (case 3 in Fig. 9) as in case 2, the high (low) peak drops down (goes up) indicating the weakening of the DB (dot-dashed line in Fig. 10), but the lag and asymmetric characteristics are not changed.

The detailed evolutions of DB impacted by TDW are presented in Fig. 11. For case 1 (Fig. 11a), the DB evolution process is similar to that without the TDW term in Fig. 3b, exhibiting a symmetric feature about the peak phase in the evolution of the DB episode. The most differences between Fig. 3b and Fig. 11a are in the different intensity of DB at any phase during the DB life cycle and zonal and meridional scales. The high/low intensity weakens in case 1 and the zonal and meridional scales of DB all lessens a little, suggesting the DB period shortens, which is coherent with the results discussed above from Fig. 10. For case 2 the developing process from the onset ($t = 3$) of DB to its peak phase ($t = 6$) resembles that in case 1, but the decay process from the DB peak phase to blocking vanishing ($t = 10$) appears very different. Compared to the DB evolution process without TDW (Fig. 3b),

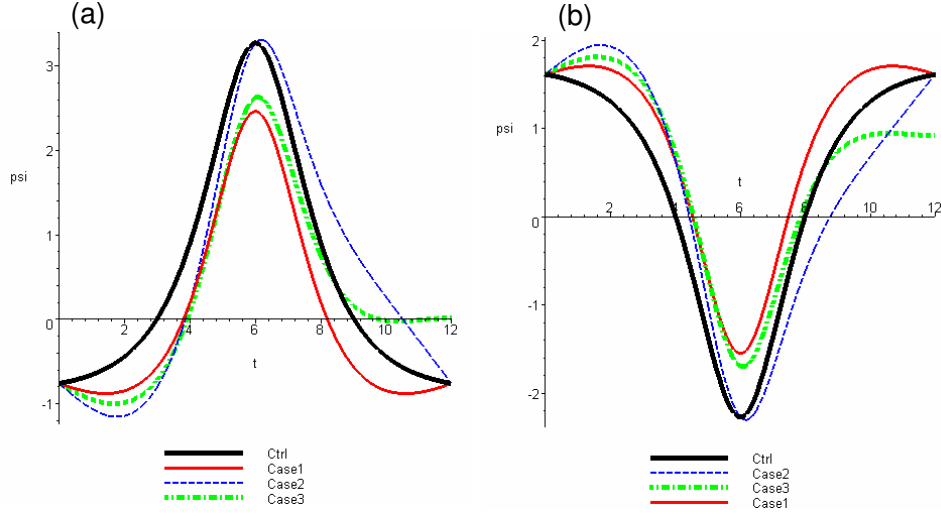


FIG. 10: The intensity of the DB high (a) and low (b) center varying with respect to time t under different types of TBW as shown in Fig. 9 during the DB life cycle. Label "Ctrl" means the case of background westerly \bar{u} without time-dependent term $a_3(t) = 0$.

the dipole center of the blocking in case 2 is stronger than that in Fig. 3b at the beginning decay stage ($t = 7, 8$). At $t = 9$ the dipole-like pattern with closed high/low centers still maintains although the streamlines become sparser in case 2, while it disappears and only shows a dipole-like envelop in Fig. 3b. At $t = 10$ the almost straight streamlines in Fig. 3b are instead of dipole-like envelop in Fig. 11b with sparser streamlines. Above all, the effect of the TDW on evolution of DB is owing to altering the DB life period and leading to the asymmetry of the DB life cycle evolution with respect to its peak phase.

IV. OBSERVATIONAL FEATURES OF DB IN THE NORTHERN HEMISPHERE

A. Data and the DB definition

The data source in this study is the NCEP-NCAR reanalysis data from January 1958 to December 1997, which uses a state-of-the-art global data assimilation system (Kalnay et al. 1996). The variables used in this study are daily mean geopotential height at 1000 and 500

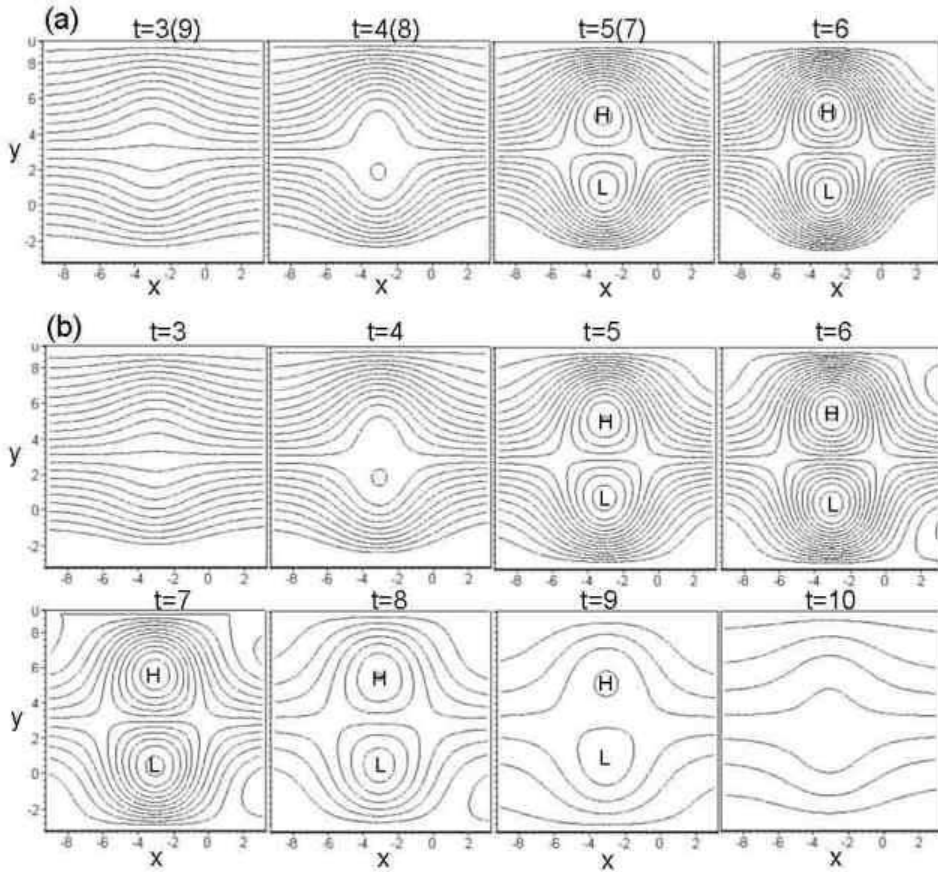


FIG. 11: The stream function patterns of DB evolution under different time-dependent westerly profiles appeared in Fig. 9. (a) Case 1; (b) Case 2. CI=0.4.

hPa and the west-east wind component at 500 hPa, on a 2.5° latitude \times 2.5° longitude grid, from $20^\circ N$ to $90^\circ N$ around the Northern Hemisphere.

Although the blocking phenomenon is well known in the meteorological community, there is no generally accepted definition of a blocking event (Lejenänd Økland 1983). Commonly used definitions can be divided into four categories of methods to identify blocking. The first is a subjective technique first put forward by Rex (1950a,b) in the 1950s. This was then inherited and modified by Sumner (1954) and White and Clark (1975). They identified the blocking events subjectively by visual inspection and then used semiobjective criteria to determine the exact dates of initiation and duration of blocking based on examination of the daily weather charts. The second category uses objective criteria first used by Elliott and Smith (1949) based on magnitude and persistence of pressure anomalies. Later, Hartman and Ghan (1980), Dole and Gordon (1983), Dole (1986, 1989), Shukla and Mo (1983), Huang (2002), and Huang et al. (2002b) extended the analysis from sea level pressure departure to the occurrence of persistent positive geopotential height anomalies at the upper level. The

useful objective criteria for identifying blocking events were designed by Lejenänd Økland 1983, using the north-south geopotential height gradient based on the coherence between the occurrence of persistent anomalous mid-latitude easterly flow and blocking. The advantage of this objective method is its simplicity for automatic calculation, and it has therefore been used widely (Tibaldi and Molteni 1990; DAndrea et al. 1998; Huang et al. 2002a). Recently, Pelly and Hoskins (2003a,b) constructed a new dynamical blocking index using a meridional θ difference on a potential vorticity (PV) surface. They reveal that their PV- θ index is better able to detect Ω blocking than conventional height field indices. Since we are focusing on dipole-type blocking, the newest PV- θ index is not suitable for us in this study.

All of the definitions of blocking mentioned above do not wholly address DB, so new criteria for identifying DB have to be established. In this study the DB is distinguished by the following criteria.

- 1) At least on pair of closed high/low contours appears simultaneously at 4 (2.5) geopotential decameters (dam) contour interval at 500 hPa (1000 hPa), with the distance between the high and low centers is no larger than 30 longitudes.
- 2) The westerlies must split into two branches at 500 hPa, and the distance between the divarication point and the meeting point is no less than 45 longitudes.
- 3) The closed high or low center lasts at least 5 days.
- 4) The moving speed of the blocking does not exceed ten degrees of longitude per day.
- 5) The high center is located at least north of $40^\circ N$.
- 6) The blocking index (BI) is no less than 20 ms^{-1} .

The BI is calculated as $BI = U_{WM} - 3 \times U_{EM} \text{ ms}^{-1}$, where U_{EM} is the maximum of the 20-point running mean of geostrophic easterlies bounded by 20 degrees of longitude in the east and west of the high center, respectively, and 30 degrees of latitude south of the high center; U_{WM} is the maximum of the westerlies south of the U_{EM} position bounded by 30 degrees of latitude. Because the easterlies south of the blocking anticyclone are usually about 3 times less than the westerlies, 3 times U_{EM} is calculated in BI. The geostrophic wind U is calculated as $U = -(g/f)\partial z/\partial y$ (f is the Coriolis parameter, g is the gravitational acceleration, and z is the geopotential height at 500 hPa). The latitude and longitude of the high center denote the position of the high, which is prescribed similarly to that of Dole (1986) as persistent positive anomalies (with respect to latitude mean) greater than 70 gpm at 500 hPa. The number of times that dipole-type blocking appears is counted and the latitude where the

high center of a dipole block is located is regarded as the meridional position of the DB.

B. Climatological features of DB and possible reasons

Many studies have derived a comprehensive set of climatological statistical characteristics of blocking anticyclones using subjective or objective techniques, including location, frequency, duration, intensity, size, and distribution (Elliott and Smith 1949; Rex 1950a,b; White and Clark 1975; Lupo and Smith 1995a; Lejenänd Økland 1983; Huang et al. 2002a; Huang 2002). Preferred Northern Hemisphere locations for blocking are the northeastern boundaries of the Pacific and Atlantic Oceans and the Ural area (Elliott and Smith 1949; Rex 1950b; Lejenänd Økland 1983; Dole and Gordon 1983; Shukla and Mo 1983; Huang 2002). For the statistical characteristics of DB, only Luo and Ji (1991) performed an observational study of dipole-type blocking in the atmosphere during 1969-84. However, the time series are too short to include the interdecadal variability of blocking (Huang et al. 2002b). The availability of the NCEP-NCAR reanalysis data (Kalnay et al. 1996) includes a considerably long time series, and so provides a solid basis for understanding behavior of the atmospheric midlatitude blocking.

In this paper, statistical features of DB in the Northern Hemisphere are investigated based on a 40-yr period data spanning from 1958C97. Results show that there are three preferable regions: the northwestern Pacific, the Atlantic, and the Ural area, where DB frequently occurred, agreement with the results of Luo and Ji (1991). The Pacific is the most preferable region, where a total of 1982 days of DB occurred, far more than the Atlantic (848 days) and Ural areas (533 days). It is interesting to note that the papers by Elliott and Smith (1949) and Rex (1950b), which were published within a year of each other, gave contradictory results on the relative frequency of blocking in the Atlantic and Pacific. White and Clark (1975), however, obtained a result that was not in agreement with Rex (1950b). In the research of Elliott and Smith (1949), they found that the total number of blocking days in central Pacific is 4 times of that in the northeastern Atlantic. Notice that the previous results did not distinguish the DB or monopole blocking, Elliott and Smiths (1949) results might include more DBs, while the statistics of Rex (1950b) may include more monopole blocks since they used different data in different periods of time or their definitions of blocking may not be exactly the same.

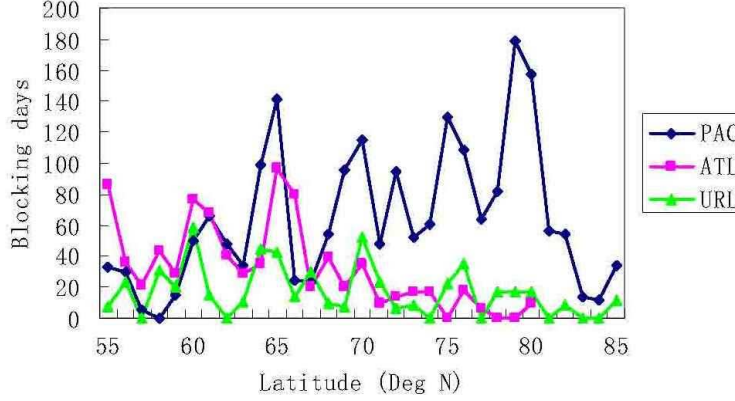


FIG. 12: The latitudinal distribution of DB over three favorable regions.

The latitudinal distribution of DB over the three favorable regions is displayed in Fig. 12. It is shown that the latitude of DB over the Pacific is mostly concentrated at $65^{\circ}N \sim 80^{\circ}N$, while the DB over Atlantic focuses at $55^{\circ}N \sim 65^{\circ}N$, about 10° southward from that in the Pacific. The Ural area has the least DB, mainly at $60^{\circ}N \sim 70^{\circ}N$, and it is also more southward than that over the Pacific.

From the statistics above it is found that the Pacific is the most favorable place for DB occurrence, but fewer blocking events (include DB and Ω blocking) occurred over the Pacific compared to the Atlantic and Ural areas (see Huang 2002). Why DB seems to prefer the Pacific? This is really a puzzling question. According to the analysis in section III, we know the intensity of the background mean westerlies is associated with the DB development. Therefore, the observational westerlies are examined first. Figure 13 displays the climatological seasonal cycle of the westerlies averaged in the high latitudes ($55^{\circ} - 80^{\circ}N$) for the Northern Hemispheric DB preferable latitudes at 500 hPa and annual mean westerly profiles with respect to latitudes averaged over three favorable regions for DB occurrence: the Pacific ($120^{\circ}E - 150^{\circ}W$), the Atlantic ($60^{\circ}W - 30^{\circ}E$) and the Ural ($30^{\circ}E - 90^{\circ}E$) areas, respectively. It is noticeable that the westerlies where the high center of DB locates preferably over the high latitudes of the Pacific region are almost all less than that over the Atlantic and Ural areas (Fig. 13a). The climatological annual mean westerly over the Pacific is about $3.25m/s$, not reaching half of that over the Atlantic ($7.35m/s$) or Ural areas ($7.77m/s$). Hence it is not strange that many more DBs occurred over the Pacific than over the Atlantic and Ural regions. From a climatological point of view, the weak westerlies are

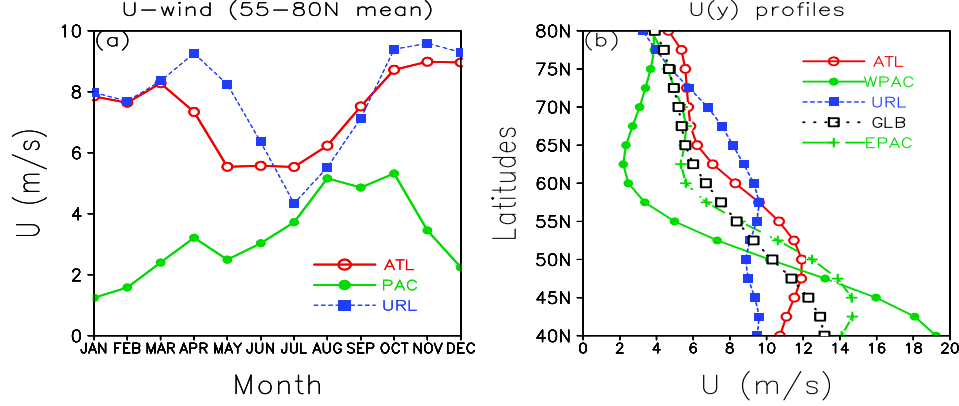


FIG. 13: Climatological seasonal cycle of westerlies (a) and westerly profiles with respect to latitudes (b) averaged over Pacific (PAC or WPAC, $120^{\circ}E \sim 150^{\circ}W$), Atlantic (ATL, $60^{\circ}W \sim 30^{\circ}E$) and Ural (URL, $30^{\circ}E \sim 90^{\circ}E$) areas. Label "EPAC" denotes the eastern Pacific averaged from 180° to $90^{\circ}W$, and "GLB" is the mean of PAC, ATL and URL.

one of the most important factors that impact the DB occurrence.

However, the weak westerly is a precondition for onset of blocking, including DB and monopole blocks (Shutts 1983, 1986; Luo and Ji 1991; Luo 1994; Luo et al. 2001). The inconsistency between DB (the most located at northwestern Pacific) and total blockings (the least occurred at northeastern Pacific) implies that the weak westerly is a necessary condition for blocks, but not a sufficient condition for DB onset. Since the westerly shears play a considerably important role in DB evolution, the annual mean westerly profiles with respect to latitudes averaged over the three DB preferable regions are also studied (Fig. 13b). The figure reveals that westerly profile over the global DB regions appears to be a weak cyclonic westerly shear from $40^{\circ}N$ to $80^{\circ}N$, which is advantageous for DB establishment at these latitudes. The Pacific has the strongest CWS from $40^{\circ}N$ to $60^{\circ}N$ and a considerably weak AWS from $60^{\circ}N$ to $80^{\circ}N$, which favors more DB produced at higher latitudes and less DB reduced at lower latitudes, corresponding to the latitudinal distribution of the DB shown in Fig. 12.

Observational studies also give the seasonal variability of global DB as shown in Fig. 14a. The numbers of DB decrease from winter (December to February) to spring (March to May),

summer (June to August), and autumn (September to November) successively. Winter is the most favorable season for DB producing, consistent with the results for total blocking by White and Clark (1975), Lejenänd *varnothing*kland (1983), Shukla and Mo (1983), and Huang (2002), but contradictory to results by Rex (1950a); while autumn is the quiet season for DB onset, which disagrees with the common statistical results for total blocking (White and Clark 1975; Lejenänd *varnothing*kland 1983; Shukla and Mo 1983; Huang 2002). The mean westerlies averaged over the three preferable DB regions in each season (Fig. 14b) indicate that the autumn westerlies are the strongest, and are associated with the least DB occurring in autumn according to the theory discussed above. The summer westerly is weakest, but does not correspond to the largest DB frequency in summer. Nevertheless, the seasonal variability of the background westerlies over the Pacific region ($120^{\circ}E \sim 150^{\circ}W$) in Fig. 14c appears to have a completely negative correlation to the seasonal cycle of the global DB occurrence in Fig. 14a. This suggests that the seasonal variation of the global DB is mostly due to the seasonal cycle of the Pacific DB, which is mostly determined by the mean background westerlies over the Pacific. For the Atlantic and Ural DB, the seasonal variability of the mean westerlies may play important but indecisive role in the DB seasonal cycle. The seasonal westerly profiles with respect to latitudes over the Pacific region of DB (Fig. 14d) show that the westerly shears are very favorable for DB establishment in winter, spring and autumn, with a CWS at $45^{\circ} - 60^{\circ}N$ and very weak AWS at higher latitudes, while in summer the AWS at $60^{\circ} - 75^{\circ}N$ seems too strong to be unfavorable for DB pattern developing. It is remarkable that among the very weak AWSs in winter, spring and autumn, the AWS in winter is the relatively strongest one, which is favorable for strong DB development, and results in the most DB occurring in winter. Therefore, the intensity of the background mean westerlies and their shear structures closely associate with the establishment of DB, leading to the northwestern Pacific being the most preferable region for DB and its seasonal variability.

V. CONCLUDING REMARKS

In this paper, a variable coefficient Korteweg de Vries (VCKdV) system is derived by considering the time dependent background flow and boundary conditions from the non-linear, inviscid, nondissipative, and equivalent barotropic vorticity equation in a beta-plane

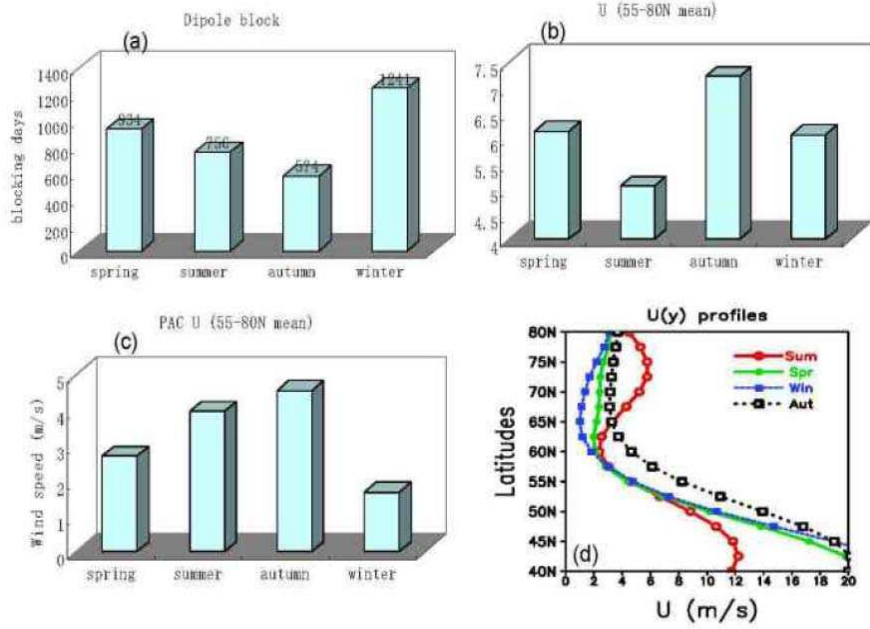


FIG. 14: Seasonal variations of (a) the number of DB days, (b) the mean westerlies averaged over the three DB preferable regions, (c) westerlies averaged over the Pacific ($120^{\circ}E \sim 150^{\circ}W$), and (d) seasonal mean westerly profiles with respect to latitude averaged over the Pacific. Label "Win" denotes winter season (December to February), "Sum" denotes summer (June to August), "Spr" denotes spring (March to May), and "Aut" denotes autumn (September to November).

channel. The analytical solution obtained from the VCKdV equation can be successfully used to explain the evolution of atmospheric dipole-type blocking life cycle. Analytical diagnoses are analyzed and three factors that may influence the evolution of atmospheric DB are investigated.

Theoretical results show that the background mean westerlies have great influence on evolution of DB during its life episode. Weak westerlies are necessary for blocking development and the high/low centers of blocking decrease and move southward and westward, the horizontal scale enlarges and meridional span reduces, as well as the blocking life period shortens with respect to the enhanced westerly.

Shear of the background westerlies also plays an important role in evolution of DB. The CWS is preferable for the development of DB, which agrees with the recent result from Luo (2005b). When the cyclonic shear increases, the intensity of DB decreases and its life period becomes shorter. Weak AWS is also favorable for DB formation, but a critical threshold shear

exists, beyond which a cutoff anticyclone from the North Pole region develops dramatically instead of an envelope Rossby soliton forming the high anticyclone center of DB. Inside the critical threshold of the anticyclonic shear, the intensity of DB increases and the life period of DB prolongs when the anticyclonic shear increases. For the role of CWS in DB evolution, our result is inconsistent with that of Luo (2005b), who revealed that an isolated vortex pair block excited resonantly by synoptic-scale eddies is more likely suppressed in an anticyclonic shear environment. The difference may lie on different nonlinear systems considered by Luo (2005b) and us. That is, Luo (2005b) considered an eddy-forced nonlinear Schrödinger Rossby soliton system in the atmosphere, while we established a nonlinear system based on a nonlinear KdV equation without forcing, and our results show that the nonlinear effect of the free atmosphere could also induce blocking circulation by its intrinsic nonlinear interaction without external eddy forcing.

Time-dependent variation of background flow in the life cycle of DB has some modulations on blocking life period and intensity due to the behavior of the mean westerlies. The effect of TDW, especially the style of TDW, reflecting interaction between the background westerlies and blocking, with the westerlies decreasing during the developing period before DB peak and increasing throughout the decay stage after DB peak, is caused by the alteration of the DB life period and leads to the asymmetry of the DB life cycle evolution.

Statistical analysis of climatological features of observed DB is investigated based on 40-yr geopotential height fields from the NCEP-NCAR reanalysis data during 1958-97. Observational results show that there are three preferable regions of DB in the Northern Hemisphere, located in the northwestern Pacific, the northeastern Atlantic and the Ural Mountain areas, in agreement with the results of Luo and Ji (1991). The number of DB days occurring over the Pacific is far larger than total of that over the other two regions, corresponding to the weaker westerlies over the northwestern Pacific and the particular westerly shear structure over Pacific. The Pacific DB prefers to be established at higher latitudes than the Atlantic and Ural regions by about 10° , which may be caused by its having the strongest CWS at mid-latitudes and weaker AWS at higher latitudes over the Pacific region. Seasonal variability of the global DB is also associated with the seasonal cycle of the mean westerlies over the Pacific and the westerly shear structure. Therefore, the intensity of the mean westerlies and the shear structure of the westerly profiles are two important conditions associated with the climatological features of the DB in the Northern Hemisphere, which may play crucial role

in the DB life cycles. The type of TDW could also impact the DB life episode concluded from analytical resolution, but it is yet to be demonstrated from the observational studies in the future.

Acknowledgments

The work was supported by the National Natural Science Foundation of China (Grants 40305009, 10475055, 1054124, and 90203001), Program for New Century Excellent Talents in University (NCET-05-0591), Program 973 (No. 2005CB422301), and Shanghai Post-Doctoral Foundation.

REFERENCES

- Berggren, R., B. Bolin, and C. G. Rossby, 1949: A aerological study of zonal motion, its perturbations and breakdown. *Tellus*, 1, 14C37.
- Butchart, N., K. Haines, and J. C. Marshall, 1989: A theoretical and diagnostic study of solitary waves and atmospheric blocking. *J. Atmos. Sci.*, 46, 2063C2078.
- Cascaval, R. C., 2003: Variable coefficient kortevég-de vries equations and wave propagation in elastic tubes. *Evolution Equations*, Goldstein, G. and Nagel, R. and Romanelli, S. (eds.), New York, NY: Marcel Dekker, 57C69.
- Charney, J. G. and J. G. DeVore, 1979: Multiple flow equilibria in the atmosphere and blocking. *J. Atmos. Sci.*, 36, 1205C1216.
- Chen, W. and H. H. Juang, 1992: Effect of transient on blocking flows: General circulation model experiments. *Mon. Wea. Rev.*, 120, 787C801.
- Colucci, S. J., 1985: Explosive cyclogenesis and large-scale circulation changes: Implications for atmospheric blocking. *J. Atmos. Sci.*, 42, 2701C2717.
- 1987: Comparative diagnosis of blocking versus non-blocking planetary-scale circulation changes during synoptic-scale cyclogenesis. *J. Atmos. Sci.*, 44, 124C139.
- Colucci, S. J. and T. L. Alberta, 1996: Planetary-scale climatology of explosive cyclogenesis and blocking. *Mon. Wea. Rev.*, 124, 2509C2520.
- Colucci, S. J. and D. P. Baumhefner, 1998: Numerical prediction of the onset of blocking: a case study with forecast ensembles. *Mon. Wea. Rev.*, 126, 733C784.
- D’Andrea, F., S. Tibaldi, and M. Blackburn, 1998: Northern hemisphere atmospheric blocking as simulated by 15 atmospheric general circulation models in the period 1979-1988.

Climate Dynamics, 14, 385C407.

Dole, R. M., 1986: Persistent anomalies of the extratropical northern hemisphere winter-time circulation: Structure. *Mon. Wea. Rev.*, 114, 178C207.

– 1989: Life cycle of persistent anomalies, part i: Evolution of 500-mb height fields. *Mon. Wea. Rev.*, 117, 177C211.

Dole, R. M. and N. D. Gordon, 1983: Persistent anomalies of the extra-tropical northern hemisphere wintertime circulation: Geographical distribution and regional persistence characteristics. *Mon. Wea. Rev.*, 111, 1567C1586.

Egger, J., W. Metz, and G. Muller, 1986: Synoptic-scale eddy forcing of planetary-scale blocking anticyclones. *Adv. Geophys.*, 29, 183C198.

Elliott, R. D. and T. B. Smith, 1949: A study of the effects of large blocking highs on the general circulation in the northern hemisphere westerlies. *J. Meteor.*, 6, 67C85.

Flytzanis, N., S. Pnevmatikos, and M. Remoissenet, 1985: Kink, breather and asymmetric envelope or dark solitons in nonlinear chains: I. monatomic chain. *J. Phys. C*, 18, 4603C4629.

Gottwald, G. A. and R. H. J. Grimshaw, 1999: The effect of topography on dynamics of interacting solitary waves in the context of atmospheric blocking. *J. Atmos. Sci.*, 56, 3663C3678.

Haines, K. and A. J. Holland, 1998: Vacillation cycles and blocking in channel. *Quart. J. Roy. Meteor. Soc.*, 124, 873C895.

Haines, K. and J. C. Marshall, 1987: Eddy-forced coherent structures as a prototype of atmospheric blocking. *Quart. J. Roy. Meteor. Soc.*, 113, 681C704.

Hansen, A. and T. C. Chen, 1982: A spectral energetics analysis of atmospheric blocking. *Mon. Wea. Rev.*, 110, 1146C1159.

Hartman, D. L. and S. J. Ghan, 1980: A statistical study of the dynamics of blocking. *Mon. Wea. Rev.*, 108, 1144C1159.

Holopainen, E. and C. Fortelius, 1987: High-frequency transient eddies and blocking. *J. Atmos. Sci.*, 44, 1632C1645.

Hoskins, B. J., M. E. McIntyre, and A.W. Robertson, 1985: On the use and significance of isentropic potential vorticity maps. *Quart. J. Roy. Meteor. Soc.*, 111, 877C946.

Huang, F., 2002: Study on the atmospheric blocking circulation over the North Pacific during winter and its connection with the mid-low latitude interaction. Ph.D. thesis, Ocean

University of China.

Huang, F., F. X. Zhou, and P. J. Olson, 2002a: Variations of the atlantic and pacific blocking anticyclones and their correlation in the northern hemisphere. *J. of Ocean University of Qingdao (English Edition)*, 1, 38C44.

Huang, F., F. X. Zhou, and X. D. Qian, 2002b: Interannual and decadal variability of north pacific blocking and its relationship to sst, teleconnection and storm track. *Adv. Atmos. Sci.*, 19, 807C820.

Illari, L., 1984: A diagnostic study of the potential vorticity in a warm blocking anticyclone. *J. Atmos. Sci.*, 41, 3518C3526.

Illari, L. and J. C. Marshall, 1983: On the interpretation of eddy fluxes during a blocking episode. *J. Atmos. Sci.*, 40, 2232C2242.

Ji, L. R. and L. Tibaldi, 1983: Numerical simulations of a case of blocking: The effects of orography and land-sea contrast. *Mon. Wea. Rev.*, 111, 2068-2086.

Kalnay, E., M. Kanamitsu, R. Kistler, W. Collins, D. Deaven, L. Gandin, M. Iredell, S. Saha, G. White, J. Woollen, Y. Zhu, M. Chelliah, W. Ebisuzaki, W. Higgins, J. Janowiak, K. C. Mo, C. Ropelewski, J. Wang, A. Leetmaa, R. Reynolds, R. Jenne, and D. Joseph, 1996: The ncep/ncar 40-year reanalysis project. *Bull. Am. Meteorol. Soc.*, 77, 437-471.

Lejenäs, H. and H. Øland, 1983: Characteristics of northern hemisphere blocking as determined from a long time series of observational data. *Tellus*, 35A, 350-362.

Long, R. R., 1964: Solitary waves in the westerlies. *J. Atmos. Sci.*, 21, 197C200.

Luo, D. H., 1994: The dynamical characters of local blocking high and dipole blocking in the atmosphere. *Plateau Meteorology (in Chinese)*, 13, 1C13.

– 1995: Solitary rossby waves with the beta parameter and dipole blocking. *Quarterly Journal of Applied Meteorology (in Chinese)*, 6, 220C227.

– 1999: Envelope soliton theory and blocking pattern in the atmosphere. *China Meteorological Press*, 113 pp.

– 2000: Nonlinear dynamics of blocking. *China Meteorological Press*, 248 pp.

– 2001: Derivation of a higher order nonlinear schrodinger equation for weakly nonlinear rossby waves. *Wave Motion*, 33, 339C347.

– 2005a: A barotropic envelope rossby soliton model for block-eddy interaction. part ii role of westward-traveling planetary waves. *J. Atmos. Sci.*, 62, 22C40.

– 2005b: A barotropic envelope rossby soliton model for block-eddy interaction. part iv:

Block activity and its linkage with sheared environment. *J. Atmos. Sci.*, 62, 3860C 3884.

Luo, D. H., F. Huang, and Y. N. Diao, 2001: Interaction between antecedent planetary-scale envelope soliton blocking anticyclone and synoptic-scale eddies: Observations and theory. *J. Geophys. Res.*, 106, 31795C31815.

Luo, D. H. and L. R. Ji, 1991: Observational study of dipole blocking in the atmosphere. *Scientia Atmospherica Sinica* (in Chinese), 15, 52C57.

Luo, D. H., J. P. Li, and F. Huang, 2002: Life cycles of blocking flows associated with synoptic-scale eddies: observed results and numerical experiments. *Adv. Atmos. Sci.*, 19, 594C618.

Luo, D. H. and H. Xu, 2002: The dynamical characters of local blocking high and dipole blocking in the atmosphere. *Journal of Ocean University of Qingdao* (in Chinese), 32, 501C510.

Lupo, A. R., 1997: A diagnosis of blocking events that occurred simultaneously in the midlatitude northern atmosphere. *Mon. Wea. Rev.*, 125, 1801C1823.

Lupo, A. R. and P. J. Smith, 1995a: Climatological feature of blocking anticyclones in the north hemisphere. *Tellus*, 47A, 439C456.

– 1995b: Planetary and synoptic-scale interactions during the life cycle of a midlatitude blocking anticyclone over the north atlantic. *Tellus*, 47A, 575C596.

– 1998: The interactions between a midlatitude blocking anticyclone and synopticscale cyclone that occurred during the summer season. *Mon. Wea. Rev.*, 126, 502C 515.

Malguzzi, P. and P. Malanotte-Rizzoli, 1984: Nonlinear stationary rossby waves on nonuniform zonal winds and atmospheric blocking, part i: The analytical theory. *J. Atmos. Sci.*, 41, 2620C2628.

McWilliams, J. C., 1980: An application of equivalent modons to atmospheric blocking. *Dyn. Atmos. Oceans*, 5, 43C66.

Michelangeli, P. A. and R. Vautard, 1998: The dynamics of euro-atlantic blocking onsets. *Quart. J. Roy. Meteor. Soc.*, 124, 1045C1070.

Mullen, S. L., 1987: Transient eddy forcing of blocking flows. *J. Atmos. Sci.*, 44, 3C22.

Pedlosky, J., 1979: *Geophysical Fluid Dynamics*. Springer-Verlag, 624 pp.

Quiroz, R. S., 1984: The climate of the 1983-84 winter: A season of strong blocking and severe cold in north america. *Mon. Wea. Rev.*, 112, 1894C1912.

Rao, N. N., P. K. Shukla, and M. Y. Yu, 1990: Dust-acoustic waves in dusty plasmas.

Planet. Space Sci., 38, 543C546.

Rex, D. F., 1950a: Blocking action in the middle troposphere and its effects upon regional climate: I. an aerological study of blocking action. *Tellus*, 2, 196C211.

– 1950b: Blocking action in the middle troposphere and its effects upon regional climate: Ii. the climatology of blocking action. *Tellus*, 2, 275C301.

Shukla, J. and K. C. Mo, 1983: Seasonal and geographical variation of blocking. *Mon. Wea. Rev.*, 111, 388C402.

Shutts, G. J., 1983: The propagation of eddies in diffluent jetstreams: eddy vorticity forcing of blocking flow fields. *Quart. J. R. Meteor. Soc.*, 109, 737C761.

– 1986: A case study of eddy forcing during an atlantic blocking episode. *Adv. Geophys.*, 29, 135C161.

Sumner, E. J., 1954: A study of blocking in the atlantic-european sector of the northern hemisphere. *Quart. J. R. Meteor. Soc.*, 80, 402C416.

Tanaka, H. L., 1991: A numerical simulation of amplification of low frequency planetary waves and blocking formations by the upscale energy cascade. *Mon. Wea. Rev.*, 119, 2919C2935.

– 1998: Numerical simulation of a life-cycle of atmospheric blocking and the analysis of potential vorticity using a simple barotropic model. *J. Meteor. Soc. Japan*, 76, 983C1008.

Tibaldi, S. and F. Molteni, 1990: On the operational predictability of blocking. *Tellus*, 42A, 343C365.

Tracton, M. S., K. Mo, W. Chen, E. Kalnay, R. Kistler, and G. White, 1989: Dynamical extended range forecasting (derf) at the national meteorological center. *Mon. Wea. Rev.*, 117, 1604C1635.

Tsou, C. S. and P. J. Smith, 1990: The role of synoptic/planetary-scale interactions during the development of a blocking anticyclone. *Tellus*, 42A, 174C193.

Tung, K. K. and R. S. Linzen, 1979: A theory of stationary long waves, part i: a simple theory of blocking. *Mon. Wea. Rev.*, 107, 714C734.

Vautard, R. and B. Legras, 1988: On the source of midlatitude low-frequency variability. part ii: Nonlinear equilibration of weather regimes. *J. Atmos. Sci.*, 45, 2845C 2867.

Vautard, R., B. Legras, and M. Deque, 1988: On the source of midlatitude low frequency variability. part i: A statistical approach to persistence. *J. Atmos. Sci.*, 45, 2811C2844.

White, E. B. and N. E. Clark, 1975: On the development of blocking ridge activity over

the central north pacific. J. Atmos. Sci., 32, 489C501.

Yoshinaga, T. and T. Kakutani, 1984: Second order k-dv soliton on the nonlinear transmission line. J. Phys. Soc. Jpn., 53, 85C92.

Zabusky, N. J. and M. D. Kruskal, 1965: Interaction of solitons in a collisionless plasma and the recurrence of initial states. Phys. Rev. Lett., 15, 240C243.